IOPscience iopscience.iop.org

Home Search Collections Journals About Contact us My IOPscience

Diffusion and trapping of Mu in the III–V nitrides

This article has been downloaded from IOPscience. Please scroll down to see the full text article.

2004 J. Phys.: Condens. Matter 16 S4721

(http://iopscience.iop.org/0953-8984/16/40/016)

View the table of contents for this issue, or go to the journal homepage for more

Download details:
IP Address: 129.252.86.83
The article was downloaded on 27/05/2010 at 18:03

Please note that terms and conditions apply.

INSTITUTE OF PHYSICS PUBLISHING JOURNAL OF PHYSICS: CONDENSED MATTER

J. Phys.: Condens. Matter **16** (2004) S4721–S4738 PII: S0953-8984(04)77581-5

Diffusion and trapping of Mu in the III–V nitrides

R L Lichti[1], **Y G Celebi**[2], **S P Cottrell**[3], **S F J Cox**[3,4] **and E A Davis**[5]

[1] Department of Physics, Texas Tech University, Lubbock, TX 79409-1051, USA
[2] Department of Physics, Istanbul University, Beyazit, 34459 Istanbul, Turkey
[3] ISIS Facility, Rutherford Appleton Laboratory, Chilton OX11 0QX, UK
[4] Department of Physics and Astronomy, University College London, WC1E 6BT, UK
[5] Department of Materials Science and Metallurgy, University of Cambridge, CB2 3QZ, UK

Received 8 March 2004
Published 24 September 2004
Online at stacks.iop.org/JPhysCM/16/S4721
doi:10.1088/0953-8984/16/40/016

Abstract

Sites and dynamics obtained for muonium (Mu) defect centres provide a good experimental model for the behaviour of the equivalent hydrogen impurities. We discuss the dynamic properties of Mu centres in the III–V nitrides focusing on features common to the three materials. Muon spin depolarization data in zero magnetic field provide motional dynamics for the Mu^+ and Mu^- charge states and field dependent longitudinal relaxation rates probe motion of Mu^0 centres. The data also show dynamics associated with metastable locations, either intrinsic to the wurtzite structure or defect related, including trapping and release transitions. A general picture of the behaviour of H in the III–V nitrides is developed from these measurements for comparison to theoretical results.

1. Introduction

The study of the defect centres created when positive muons are implanted into a semiconducting material has historically provided the vast majority of experimental information on the behaviour of isolated hydrogen impurities. Muonium behaves in essentially all aspects as a very light hydrogen isotope, generally occupying the same interstitial sites and undergoing the same chemical interactions as obtained for H or D impurities. Because of the short muon lifetime of 2.2 μs and the extreme sensitivity of the standard muon spin research (μSR) tools, it is far easier to obtain data on Mu than on the equivalent H or D centres. Consequently, muonium results have provided important checks on theoretical modelling of the sites and other properties of isolated hydrogen impurities [1].

Due to the short lifetime, observing the results of interactions of Mu with other defects or impurities has been much more difficult than for H or D. However, using the temperature dependence of motion and transition dynamics, various interactions associated with hydrogen passivation reactions and the dissociation of the resulting defect complexes have been directly

 © 2004 IOP Publishing Ltd Printed in the UK

observed for muonium in a few materials, most notably the Mu–Zn interactions in p-type GaAs and GaP [2, 3].

GaAs can also provide an excellent case study for the vastly different motional properties expected for the three charge states of hydrogen [2, 4–6], as well as for the specific μSR techniques best suited to examining these dynamics. Both Mu^+ and Mu^- are diamagnetic centres and are usually indistinguishable in spin precession spectroscopy; however, in n-type and p-type GaAs the linewidth or Gaussian relaxation rate (σ) of the diamagnetic spin precession signal has vastly different temperature dependences [6]. Although the low temperature rate constant is nearly the same, $\sigma(T)$ shows motional narrowing above 200 K for Mu^+ which dominates in p-type samples, but motion on the microsecond μSR timescale occurs only above about 550 K for Mu^- as observed for high concentration n-type conditions. Depolarization data in zero magnetic field, which are more sensitive to slow hopping motion, yield a barrier for Mu^- thermal motion of 0.73 eV [5] compared to about 0.15 eV on average for Mu^+ [2]. However, the zero-field data show a change in Mu^+ dynamics just above the onset, interpreted as a change in the dominant Mu^+ site and the path involved [7]. Both the transverse-field spin precession and zero-field depolarization techniques are sensitive to motion of these diamagnetic muonium centres because III–V host atoms have nuclear dipole moments, leading to randomly directed local contributions to magnetic fields at the muon sites which are averaged toward zero for increasingly rapid motion among equivalent crystallographic locations.

In the case of paramagnetic Mu^0 centres, the interaction of the muonium electron with these neighbouring host nuclear spins produces a contribution to the Mu^0 hyperfine interactions that provides the sensitivity to motion. The random variations in nuclear hyperfine fields due to motion are best sensed via the relaxation rates in magnetic fields oriented parallel to the initial muon spin direction. Longitudinal relaxation data on GaAs show that a metastable Mu^0 centre is very mobile on the microsecond timescale moving rapidly among the tetrahedral interstitial regions of the zinc-blende structure at all temperatures, via quantum tunnelling at low T and thermal hopping at high T with a minimum hop rate of roughly 200 MHz near 80 K [4]. The lowest energy Mu^0 location is at a bond-centre (BC) site in most cubic semiconductors. This Mu^0_{BC} centre remains static in GaAs up to the highest temperature where it is seen, roughly 160 K. This very brief summary of results in GaAs demonstrates that diffusive properties of Mu and the equivalent H impurities are highly dependent on the charge state and that metastable locations may be critical to motional properties. The possibility of charge state transitions and paths that do not necessarily include the lowest energy sites of a given charge state need to be included when modelling diffusion of hydrogen in semiconducting materials.

In this paper, we present results on the motional dynamics of the various muonium defect centres observed to date in the III–V nitrides. Many of these results have been previously presented in conference papers focusing on individual Mu centres in specific nitride materials. Here we discuss all of these results on Mu dynamics, along with additional relevant data, in order to present a more comprehensive picture. The experimental results for muonium allow us to construct a general model of the motional properties of hydrogen in the III–V nitrides for comparison to results from theoretical calculations. The nitrides have the hexagonal wurtzite structure with a 2H stacking sequence in which each atom has a tetrahedral bond arrangement. Bond lengths are slightly different parallel and 'perpendicular' to the hexagonal c-axis. This structure offers many more possible sites for Mu or H than does the cubic zinc-blende structure of standard III–V compounds. The final section of this paper summarizes a model of hydrogen behaviour in the nitrides which can be constructed based on the experimental results for muonium as interpreted in light of theoretical modelling for hydrogen.

The theoretical models indicate that H or Mu is a strongly negative-U defect with deep donor and deep acceptor defect states and compensating electrical properties in AlN and GaN,

similar to many other semiconducting materials, but that it should only function as a shallow donor in InN [8]. The finding of negative-U behaviour implies that a neutral charge state never dominates under thermodynamic equilibrium conditions. However, immediately after muon implantation and thermalization, the non-equilibrium state mix that allows investigation of metastable sites that are long lived on the experimental μSR timescale will also often include any of the non-equilibrium charge states that are allowed for each occupied site.

The statistical framework for analysis of μSR results is drastically different from the equilibrium population treatments commonly used for interpreting typical data on defects in semiconductors. The as-implanted site and charge state mix are very far from equilibrium, and equilibrium populations are essentially never reached within the roughly 15 μs maximum time available experimentally. The zero-time mix of states is governed by muon thermalization processes on a sub-picosecond timescale and does not depend significantly on sample temperature; however, any transitions that occur faster than tens of nanoseconds will modify which states are observed. Transitions that move the system toward equilibrium are detected as temperature dependent amplitudes as transition rates are tuned through the roughly 0.1–10 MHz sensitivity window, with the precise range dependent on signals for the initial and final states for any specific experimental technique. If a transition out of a particular state is observed, we consider that state to be 'metastable', particularly when there is no evidence of return to the initial state. There are almost no situations in the nitrides where we observe bi-directional transitions for the isolated Mu defect; thus we have no access to the relative energies of various states, except to say which one is more stable. What we do have access to are the barriers associated with the various transitions. With respect to comparisons with theory, the muonium data more directly probe the calculated enthalpy landscape than do equilibrium population data. Differences in the numbers of equivalent locations for two states which contribute to entropy terms affecting relative populations, will show up in prefactors to Mu transition rates reflecting the possibility of multiple paths out of a specific state. While we do observe various charge state transitions, this paper concentrates on properties of the individual charge states, Mu^+, Mu^0, or Mu^-.

Experimentally, two distinctly different types of centres have been identified in the nitrides for each of the three Mu charge states [9, 10]. Avoided level-crossing resonances (lcr) involving the nuclear quadrupole splittings of Ga near neighbours identify two separate sites for Mu^- centres in unintentionally n-type GaN at the typical mid-10^{16} cm^{-3} electron concentration, as well as in doped samples with two to three orders of magnitude higher and lower concentrations [11, 12, 10]. Figure 1(a) shows the full spectrum for GaN at a temperature where all of the Mu^- and Mu^+ lcr lines have significant amplitude, along with the separation into individual components. The temperature dependence verifies the presence of all of these lines, even though that may not be obvious when looking at results for a single temperature. The two Mu^- sites are identified as the Ga antibonding (AB) locations (see figure 2). One strong line per Ga isotope is from the $AB_{\parallel}$(Ga) location, which is found to be metastable, with the Ga–Mu^- direction parallel to the c-axis. We have referred to this as a 'cage' site; it lies in a region that is blocked along the c-axis by the 2H stacking sequence. The lower energy location is assigned to $AB_{\perp}$(Ga) and yields the weaker doublet per Ga isotope in figure 1(a). This site lies opposite the 'perpendicular' N–Ga bond giving a Ga–Mu direction oriented at $\sim 70°$ to the axis, with three such sites from different Ga atoms lying quite close together. These locations lie in the unblocked c-axis channels provided by the 2H stacking. The lcr spectra for these 'channel sites' may not in fact distinguish between three separate $AB_{\perp}$ locations and a single central site equidistant from the three Ga atoms (see relevant discussion in the next section).

In each of the three nitrides (InN, AlN, and GaN) we have assigned a nitrogen-related avoided level-crossing resonance (see figure 1) to a static Mu^+ centre [13, 7, 10]. In GaN

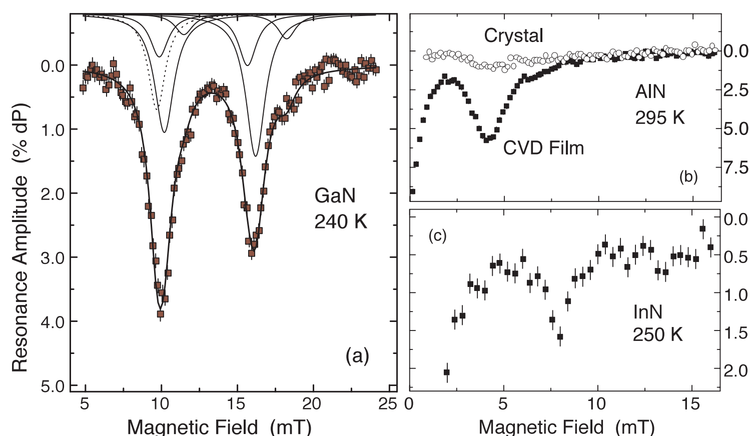

Figure 1. Examples of avoided level-crossing resonances for stationary diamagnetic muonium centres in the III–V nitrides showing spectra for one Mu^+ (N-related, broken curve) and two Mu^- (Ga-related, solid curves) sites in GaN (a). The N-related features in AlN (b) and InN (c) imply Mu^+ at either intrinsic or defect-related trap sites.

(This figure is in colour only in the electronic version)

the characteristics of this state led us to assign the $AB_{\parallel}(N)$ 'cage' site to this static Mu^+ state [10]. In AlN vastly different amplitudes for this signal in different samples and the very low occurrence at low temperatures in a single crystal suggest that this signal is from a defect-related trap site. In InN we have concluded that there is probably more than one static Mu^+ location; thus perhaps both the intrinsic $AB_{\parallel}(N)$ site and a defect-related state may be present. In addition to these static Mu^+ centres, the relaxation signature of a mobile diamagnetic centre exists at most temperatures in all three nitrides. We have associated this signal with the lowest energy Mu^+ state in each case. Arguments supporting that assignment are based in part on its motional characteristics; details are discussed further in the theoretical background and data analysis sections which follow.

A separate static zero-field depolarization signal has been identified for each of the diamagnetic states for which a level-crossing resonance was observed [10, 15, 14]. The association in each case is based on the temperatures at which dynamic features begin to appear in both the lcr and the depolarization functions. The zero-field signal separation and identification are discussed further in the section on data and analysis and are critical to assigning observed dynamics to specific Mu charge states and sites.

A shallow donor Mu^0 spin precession signal [17] with a very small hyperfine constant and its associated zero-field depolarization signature [14] were identified in InN. Ionization of this state below 60 K feeds into the depolarization signal of the Mu^+ ground state [18], providing strong experimental evidence that the ground state of Mu, and by inference H, has shallow donor properties in InN. This is the only neutral centre either directly observed or inferred in InN, a result that is consistent with the theoretical conclusions cited above [8]. In AlN no Mu^0 hyperfine spin precession signal has yet been seen; however, an atomic-like neutral state with nearly the full vacuum hyperfine constant is inferred from repolarization (or hyperfine decoupling) curves [16]. Longitudinal relaxation rates for the fraction of the muon spin polarization associated with this Mu^0 centre yield information on its motion. A complete analysis of these data is ongoing and will be presented elsewhere, but preliminary results [15] on the basic motional properties of Mu^0 in AlN will be discussed here. The

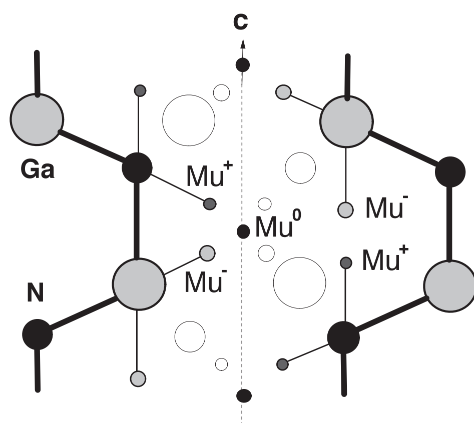

Figure 2. Sites identified for muonium centres in GaN: two Ga-related sites for Mu^-, $AB_{\parallel}$ and $AB_{\perp}$; two N-related AB sites for Mu^+, and a central channel site for Mu^0 are explicitly shown. Open symbols are for out of plane atoms and $AB_{\perp}$ sites.

situation concerning neutral muonium centres in GaN is somewhat more complicated; both types of Mu^0 states are apparently present. A Mu^0 precession signal with a very small hyperfine interaction characteristic of a shallow state is present up to about 30 K [19], and repolarization curves imply a relaxing atomic-like Mu^0 present to fairly high temperatures [10], but again no precession signal has yet been observed for this neutral centre. So far we have no definitive results on motional properties or on which state may represent the lowest energy location for Mu^0. However, initial results for the shallow centre in GaN suggest that it is probably not associated with the lowest energy Mu^+ state.

2. Theory results: sites and diffusion paths for hydrogen

A significant amount of theoretical work has been done on H in GaN due to its importance to incorporation of p-type dopants and the necessity of post-growth treatments to activate those acceptors by driving off the passivating hydrogen. In general, because of the ionicity in the Ga–N bond, the positive charge state will be strongly attracted to the nitrogen, while both the neutral and negative charge states will occupy sites closer to the Ga atoms. Much of the early theoretical work on the locations and formation energies of H impurities in GaN is summarized in [20]. We briefly summarize the most recent theoretical conclusions for comparison to the experimental results we have obtained on Mu in the nitrides. Figure 2 shows some likely sites for H in the wurtzite crystal structure.

Most authors find that H^+ bonds to a nitrogen, with one of the two inequivalent bond-centre (BC) sites or the $AB_{\perp}$(N) location having the lowest energy. Energy differences between these three sites appear to depend on details of the precise methods and basis sets used in the calculations. The most recent results [21], which use the generalized gradient approximation (GGA) of density functional theory, identify four distinctly different local minima for H^+, providing a total of eight sites associated with any N atom. The $BC_{\parallel}$ site has the lowest formation energy in this calculation, followed by the (3) $AB_{\perp}$ and (3) $BC_{\perp}$ sites at 0.21 and 0.22 eV higher, respectively, with an additional site at the $AB_{\parallel}$ position 0.39 eV above the lowest energy H^+ location. There is a strong bond to N for H^+, but with relatively low energy reorientation among the eight minima per N atom, with a maximum barrier of slightly over 0.4 eV between the lowest ($BC_{\parallel}$) and highest energy ($AB_{\parallel}$) bond orientations. That work also

discusses two paths for H^+ diffusion with barriers of 0.9 and 1.0 eV and concludes that the diffusion will be faster perpendicular to the c-axis than along that axis.

These theoretical results [21] find only a single minimum for either H^0 or H^- and place both sites on the central axis of the unblocked wurtzite channels parallel to the c-axis with the H^- closer to Ga planes than H^0. This particular calculation did not find a local minimum for H^- at $AB_{\parallel}$ where we claim a metastable Mu^- site. Three $AB_{\perp}$(Ga) sites are effectively merged to yield the obtained central channel location for H^-; although some earlier calculations [20] found separate $AB_{\perp}$ low energy sites for H^-, as observed for Mu^-. Both the neutral and negative charge states are predicted to diffuse along the c-axis within the channels, while H^- also has a second path that yields motion in the perpendicular direction. The diffusion barrier from the CGA results is lowest for H^0 at 0.5 eV, and highest for H^- at 1.4 and 1.5 eV for the two paths [21].

According to these theoretical results, the lowest energy motion should be reorientation of the N–H^+ bond among a subset of sites attached to a single nitrogen atom with an energy of $\sim$0.2–0.25 eV. The zero-point vibrational energy for the H^+ bound to N is nearly 0.2 eV based on calculated frequencies [21]. Thus, the increase in zero-point energy for Mu compared to H is most probably sufficient to produce a Mu^+ state that averages the lower energy H^+ sites. A Mu^+ ground state that is spread out due to zero-point motion, or that samples several local sites via quantum tunnelling, plus a single metastable $AB_{\parallel}$(N) site, would be fully consistent with our experimental results.

3. Data and analysis

For the diamagnetic muonium states (either of the charged centres, Mu^+ or Mu^-, or a bound defect-related complex with no unpaired electrons), the data from which information on motion is most easily extracted are from muon spin depolarization measurements in zero applied magnetic field. If these centres are stationary, the depolarization curve is given by the zero-field Gaussian Kubo–Toyabe (KT) function

$$p_s(t) = P_0\left\{\tfrac{1}{3} + \tfrac{2}{3}\left[1 - \Delta^2 t^2\right]\exp\left(-\tfrac{1}{2}\Delta^2 t^2\right)\right\} \tag{1}$$

where the static rate constant Δ is determined by the second moment of local fields at the muon site arising from dipole moments of neighbouring nuclei. These fields are randomly directed, so on average one third of the local-field components lie parallel to the initial muon spin direction, leading to the long time 'recovery' of 1/3 of the initial polarization P_0 associated with that state. The lowest temperature curve in figure 3(a) is best fit with a static KT function implying a stationary diamagnetic centre.

When a diamagnetic centre begins to move among equivalent sites with a mean hop rate ν, the dynamic form of the Kubo–Toyabe relaxation becomes the appropriate depolarization function. Within a model that assumes instantaneous site-to-site hops, the dynamic version is obtained from the static function as

$$P_{ZF}(t) = p_s(t)\,e^{-\nu t} + \nu\int_0^t p_s(\tau)\,e^{-\nu\tau}\,P_{ZF}(t-\tau)\,d\tau. \tag{2}$$

In order to experimentally obtain the proper hop rates it is commonly necessary to initially get the correct value of Δ from a temperature region where there is no motion and then treat this parameter as fixed when fitting data from the motional regime.

There are other sequences of events which will each yield their own specific type of modification to the depolarization function. In zero field a metastable to stable site-change transition is most easily seen as a temperature dependent variation in the amplitudes for the depolarization functions associated with the two states involved. Trapping of a mobile centre

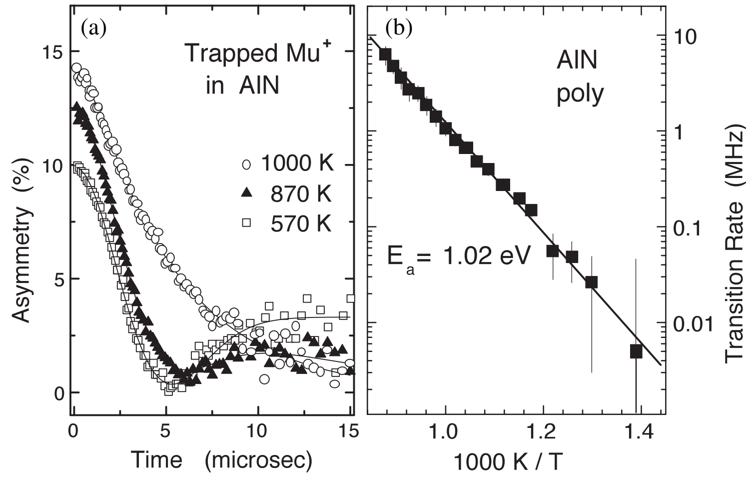

Figure 3. Muon spin depolarization data in zero applied magnetic field (a) are sensitive to the onset of dynamics for diamagnetic centres, Mu^+ or Mu^-. The static relaxation rate constant and hop rates or site-change rates (b) can be extracted. Displayed data are for the trapped Mu^+ state in polycrystalline AlN.

by a defect or other impurity in general yields a more complicated expression. Here we could in principle use the approach of [5] in which expressions are given for both trapping and de-trapping transitions. For trapping at low density stationary defects, the trapping rate is controlled by diffusion of the Mu centre to the trap and in the appropriate limit of fast diffusion one has $P_{ZF}(t) \sim 1$ which simplifies the equations. In the case of de-trapping, one can assume that the dissociation of a defect-related complex returns the Mu state to that of the rapidly diffusing centre that was originally trapped and for which no depolarization occurs. For the assumption of very fast diffusion, the appropriate expressions in a strong collision approach are as follows: for trapping at a rate of ν_r one gets a relaxation function given by

$$R(t) = e^{-\nu_r t} + \nu_r \int_0^t e^{-\nu_r \tau} q(t-\tau)\,d\tau \tag{3}$$

and for release from the trap at a rate ν_d one obtains a depolarization function of

$$D(t) = q(t)\,e^{-\nu_d t} + \nu_d \int_0^t e^{-\nu_d \tau} q(\tau)\,d\tau \tag{4}$$

where in each case $q(t)$ is the depolarization function for the trapped Mu state, typically a static KT function (equation (1)) with its own characteristic rate constant Δ_T. These are two of the simpler situations but illustrate an appropriate approach to various forms of transition dynamics.

In the case of the III–V nitrides there is nearly always more than one Mu state involved and often more than one type of transition in play at a particular temperature. Instead of using depolarization functions designed to treat specific types of transition sequences, we chose a different approach. Specifically, we used either the static or motional dynamics form of the KT depolarization function, with a different Δ associated with each identified state. The temperature dependent amplitudes for the various signals and whether a particular signal showed dynamic features provided the clues for identifying the states and dynamics. We choose GaN as the most complicated example to discuss our procedures for separating the zero-field depolarization signatures and assignment of the different relaxation functions to specific Mu centres. We relied heavily on correlations between the temperature dependences

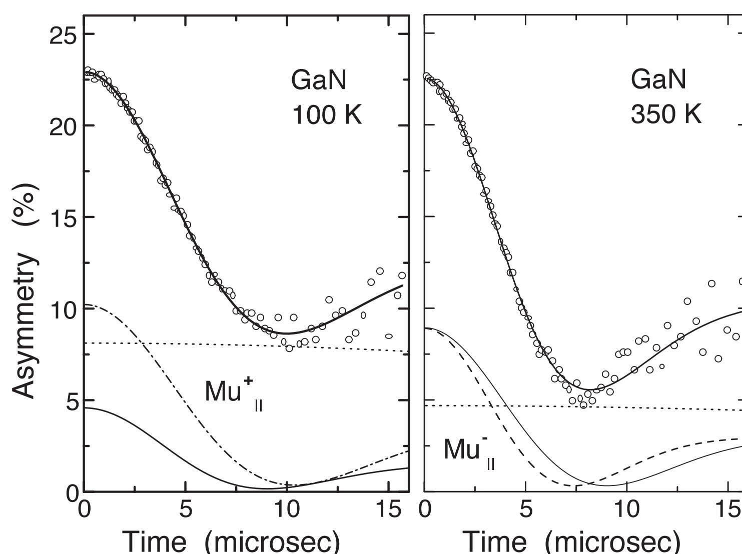

Figure 4. Separation of the zero-field depolarization curves into signals associated with specific diamagnetic Mu centres. The solid curves represent Mu^- at $AB_\perp(Ga)$ and the dotted lines are the mobile Mu^+ centre. The third signal (labelled) is Mu^+ at $AB_\|(N)$ at 100 K but Mu^- at $AB_\|(Ga)$ at 350 K.

of the zero-field depolarization results and temperature dependences of the lcr spectra for the same samples. Additionally, we examined both types of data in three GaN samples with quite different n-type concentrations to verify that trends regarding which Mu centres were more important made sense. The same four relaxation signals were seen up to 600 K in all three GaN samples but with different relative amplitudes, especially at higher temperatures as the system comes closer to thermal equilibrium on the μSR timescale.

In discussing separation of the zero-field (ZF) depolarization signals, we begin with the differences between the curves at 100 and 350 K shown in figure 4. On the basis of the lcr results at these temperatures, we expected to find three separate static KT depolarization functions, one common to both temperatures, plus two others with only one of these present at each temperature. The lcr data implied Mu^- at the $AB_\perp(Ga)$ site present throughout this range, with the second state being Mu^+ at the $AB_\|(N)$ site for 100 K but Mu^- at the $AB_\|(Ga)$ site for 350 K. The zero-field data visually imply a static KT component and a weakly relaxing component at both temperatures. Initial fits to a weakly relaxing Gaussian plus a single static KT function did not do a particularly good job, nor did using a Lorentzian for the weakly relaxing component or a single dynamic KT function for the 'static' component. However, a three-function fit with a weakly relaxing Gaussian and two static KT components provided very good fits up to above 400 K in all three GaN samples. Additionally, the rate constants obtained were quite similar and had similar temperature dependences in all three samples. For the KT components, one value of Δ was present throughout this range and the second value showed a change between 150 and 300 K in each case, generally consistent with the lcr results. We then assigned a Δ to each state based on averages over the temperature range where each was present and away from any transitions. This averaging was done separately for each sample and the results agreed to within statistical errors for all three static centres. The data were then refitted with all signals present, but with the Δ values fixed as listed in table 1. Various checks were performed to identify dynamic features in the depolarization functions and their respective amplitudes.

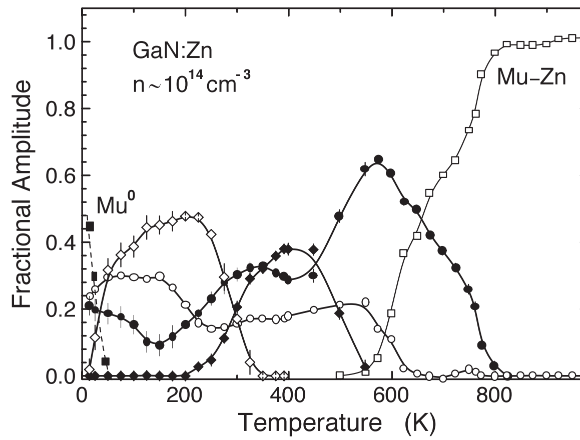

Figure 5. Amplitudes for the zero-field depolarization functions associated with the various Mu defect centres. Circles are $AB_{\parallel}$ sites and diamonds are $AB_{\perp}$ sites, filled symbols are for Mu^-, open symbols are for Mu^+. The squares at high and low temperatures are tentatively identified as labelled.

Table 1. Zero-field depolarization signals identified for diamagnetic muonium defect centres in the III–V nitrides, Mu state assignments, the depolarization function and the low temperature rate constant, and the correlated lcr signal or other information.

Material	State	Site	Function	Rate (kHz)	Notes
GaN	Mu^-	$AB_{\parallel}$(Ga)	s-KT	246 ± 5	Ga-lcr EFG $\parallel$ **c**
	Mu^-	$AB_{\perp}$(Ga)	d-KT	192 ± 3	Doublet Ga-lcr
	Mu^+	$AB_{\parallel}$(N)	s-KT	167 ± 5	N-lcr EFG $\parallel$ **c**
	Mu^+	Mobile	Gaussian	12–25	Sample dependent
	Mu–Zn	Zn^- trap	s-KT	110 ± 5	600–1000 K
AlN	Mu^+	Defect trap	d-KT	326 ± 7	N-lcr
	Mu^+	Mobile	Gaussian	20–60	Sample dependent
	Mu^+	High T trap	s-KT	$\geqslant$400	$T \geqslant 1050$ K
InN	Mu^+	Trap(s)	s-KT	294 ± 7	N-lcr; average signal
	Mu^+	Mobile	Gaussian	90–150	Sample dependent

Figure 5 shows the complete temperature variation for all of the ZF depolarization signals identified in the lowest concentration of three n-type GaN samples examined. This sample was doped with Zn to yield high resistivity and thus was partially compensated but apparently still n-type with Mu^- dominating up to 600 K. The results above 600 K are unique to this sample and will be discussed later. The basic behaviours below 600 K were very similar in all three samples, except that the Mu^- fractions increased with n-type concentration. Both lcr and ZF data suggest that at the highest temperatures all of the muons eventually produce Mu^- in the highest concentration $\sim 10^{18}$ cm^{-3} Si-doped material. Data on nominally undoped $\sim 10^{16}$ cm^{-3} GaN were not as clear regarding the high temperature Mu^- to Mu^+ ratio. If our interpretation of the high temperature state as a Mu–Zn complex in the Zn-doped material is correct, this result implies that a switch from Mu^- to Mu^+ occurs between 600 and 750 K for the high resistivity case.

In AlN and InN, no Mu^- signals were found. In both cases, there were two Mu^+ signals [13, 15, 14]: one slowly relaxing, implying a mobile centre; and one with static KT characteristics at lower temperatures with an amplitude and T dependence that correlates

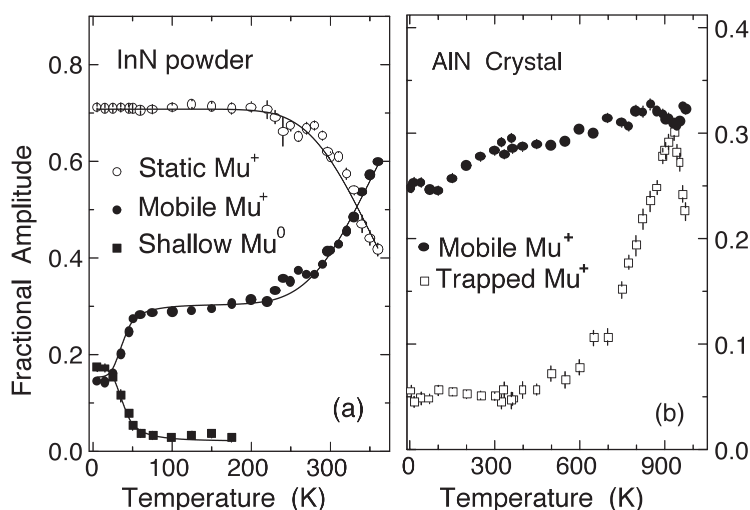

Figure 6. Zero-field amplitudes for the Mu defect centres in InN (a) and AlN (b) are identified as labelled. Data on a second InN powder sample confirm completion of the transition to the mobile Mu^+ state. For AlN films and small crystallites the amplitude for the trapped Mu^+ signal was large and sample dependent.

well with the lcr signals in figures 1(b) and (c). Figure 6 shows the ZF amplitude variations for an AlN single crystal and one of the powdered InN samples investigated. The third signal for InN, present only below about 60 K, is associated with the Mu^0 charge state of the shallow donor. These data were crucial to our claim [18] that the shallow donor site in InN is related to the mobile Mu^+ centre rather than one of the static metastable or trap sites for Mu^+.

Table 1 identifies the zero-field depolarization signals associated with the various diamagnetic muonium centres observed in the III–V nitrides, listing the function used for that signal and the static or low temperature depolarization rate constant. In several cases no dynamic features were seen except for temperature dependent amplitudes; these signals are listed as 's-KT' meaning that only the static form of Kubo–Toyabe relaxation (equation (1)) was needed, while those which did show dynamics in the shape of the depolarization function are listed as 'd-KT' meaning that the dynamic version (equation (2)) was required over some temperature region. In the following sections, we discuss motion of the lowest energy Mu^+ and Mu^- defect centres and various transition dynamics inferred from these data and a few important results on Mu^0 centres.

4. Preliminary results for Mu^0 centres

There is an extra depolarization signal below ∼50 K in the data sets for several GaN samples (see figure 5), which we believe to be due to a Mu^0 centre. This signal was modelled as a fast relaxing Gaussian in the results displayed in figure 5, although that choice was rather arbitrary. If the resulting signal separation properly reflects the actual dynamics and the state assignment is correct, then these data imply a shallow Mu^0 centre which ionizes into the metastable Mu^+ located at the $AB_{\|}$ site. This would be consistent with hyperfine anisotropy aligned with the c-axis, as has been assigned based on the orientation dependence of the shallow Mu^0 spin precession signal [19]. Therefore, an appropriate tentative conclusion is that this shallow Mu^0 centre is at a metastable 'cage' location rather than representing the lowest energy state for Mu^0

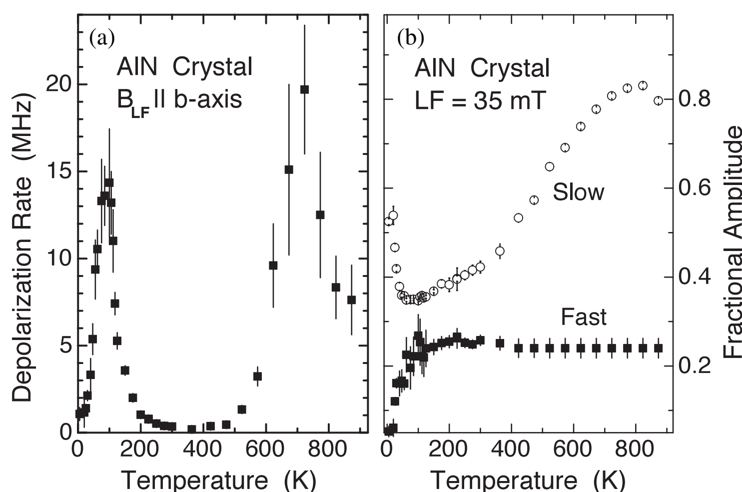

Figure 7. Longitudinal relaxation peaks (a) for single-crystal AlN imply rapid motion of a Mu^0 centre. Amplitudes (b) of the non-relaxing 'slow' component correlate well with the diamagnetic spin precession, static zero-field signal and lcr amplitudes.

which is expected to reside in the wurtzite channels. However, it should be emphasized that this is the least well characterized of all the zero-field depolarization signals observed in GaN.

Figure 7 shows some of the longitudinal depolarization results for a single-crystal sample of AlN from which we have extracted information regarding the diffusion and trapping of an atomic-like Mu^0 centre [15]. There are additional longitudinal data at several other field strengths, along with detailed repolarization curves at several temperatures. Analysis to assign a consistent set of Mu^0 hyperfine parameters and to extract the proper diffusion and conversion rates is ongoing. However, the preliminary results identify the basic behaviour of atomic-like Mu^0 centres with respect to motional properties and rates for conversion into a different state. Inferences concerning diamagnetic Mu centres drawn from the longitudinal results correlate well with those from the lcr spectra and pertinent spin precession and zero-field data on the same sample. General features show tunnelling characteristics for Mu^0 at temperatures below 300 K where the minimum hop rate occurs, plus a region of activated motion with a low prefactor contributing from about 250 to 500 K and a high temperature region with a significantly higher activation energy and prefactor. Figure 8 displays the preliminary hop rates associated with the two regions of activated motion. On the basis of the characteristics observed, the intermediate range (figure 8(b)) is most probably thermally assisted tunnelling, while the high temperature motion (figure 8(a)) yields parameters typically associated with ordinary thermal motion.

5. Motion and transitions for diamagnetic Mu centres

Rather than trying to treat the complicated dynamics observed in GaN by fitting to relaxation functions that incorporate transition processes and mix the Mu states, we chose to define separate relaxation functions for each observed muonium centre as already discussed. Transitions among these centres show up as temperature dependent amplitudes for these separate depolarization functions. In cases where dynamics are due to simple site-to-site motion or where the transitions include revisiting the same state, the depolarization functions require the dynamic version of Kubo–Toyabe. If amplitudes do not show changes correlated with the onset of dynamics, we assume that this represents motion among the equivalent sites

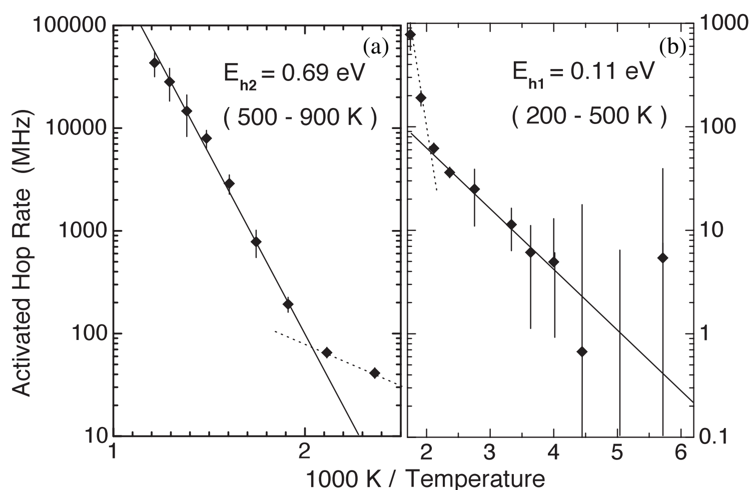

Figure 8. Hop rates for Mu^0 extracted from the longitudinal relaxation data on single-crystal AlN imply two regions of thermally activated motion above 250 K as shown here, plus tunnelling behaviour at low temperatures.

for a single centre. When the amplitudes decrease at the onset of the dynamics, we assume a transition out of that state, such as a de-trapping transition, but that the same type of centre is re-formed as a result of diffusion of an intervening mobile state and subsequent re-trapping at a similar site. For example, the onset of dynamics for Mu^- centres at $AB_\perp$ in GaN is characteristic of simple motion [11, 12]. Amplitude changes do imply transitions into and out of that state at temperatures fairly well separated from the motion onset, but the depolarization function shows consistent motion-related parameters across the entire region. We begin the discussion of specific results for the diamagnetic Mu centres with the motional properties related to the low energy Mu^+ and Mu^- sites.

Thus far Mu^- has only been seen in GaN samples and we assigned the lowest energy location to the $AB_\perp$ site associated with a Ga atom as discussed earlier. This state is represented by the filled circles in figure 5. The amplitude of this signal stays large to the highest temperatures in the two higher concentration samples. Figure 9(a) displays the site-to-site hop rates obtained from fitting this signal to the dynamic Kubo–Toyabe function with $\Delta = 236$ kHz as obtained in the static region below $\sim$400 K. Similar data from the highest concentration sample [12] gave a barrier of 0.65 ± 0.02 eV compared to 0.63 ± 0.04 eV from the results shown here and 0.6 ± 0.1 eV from broadening of the lcr linewidth for the same Zn-doped GaN sample. The more precise value of 0.65 eV comes from the sample with the largest Mu^- fraction and the least interference from competing transition processes, and thus represents the cleanest measurement of Mu^- motion in GaN.

The low energy Mu^+ centres in GaN and AlN are characterized by very weakly relaxing zero-field depolarization signals. The relaxation rates are sufficiently small that some form of motion is almost certainly required to average the local fields expected at any of the predicted sites if this centre were stationary. The relaxation rates are essentially constant up to above room temperature in both materials and decrease at higher temperatures, implying more complete motional narrowing. These features suggest tunnelling at low temperatures consistent with our discussion in the theory section of possible reorientation of the strong N–Mu^+ bond among several low energy positions surrounding a single N atom. We had earlier suggested local motion among the three closely spaced $AB_\perp$ sites related to three separate nitrogens [10, 13];

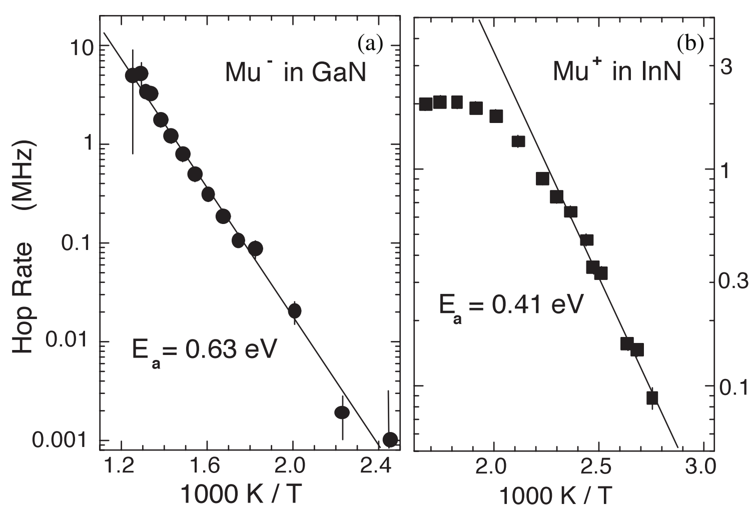

Figure 9. Hop rates for the lowest energy Mu^- centre in GaN (a) and for the low energy Mu^+ centre in InN (b). The saturation of hop rates in the InN data imply trapping of the mobile Mu^+ centre.

however, theoretical results [21] strongly favour the single-nitrogen picture. We still favour the $AB_\perp$ locations for reorientational tunnelling because motion among these sites requires minimum rearrangement of other atoms, but have no experimental data with which to test any site preference. Only the $AB_\parallel$ position seems to be excluded by specific site assignment as a metastable location in GaN based on lcr results. We have estimated the tunnelling rate at 5–10 and 2–5 MHz in GaN and AlN respectively using estimated local dipolar fields at the $AB_\perp$ positions, but this is an extremely rough estimate for both the expected fields and the resulting reorientation rates. The reduction of relaxation rates at higher temperatures is sample dependent and not very well characterized due to competing changes in other signals that could easily generate false features in the weakly relaxing component if not quite modelled correctly. However, the more complete motional narrowing observed for Mu^+ between 350 and 500 K for all three nitrides probably means a switch from local tunnelling to activated diffusive motion. We have not yet obtained consistent or reliable thermal barriers related to the high temperature activated Mu^+ motion in either GaN or AlN.

In InN, the lowest energy Mu^+ centre has a larger relaxation rate than found in the other nitrides [14], implying a slower reorientation rate estimated at less than 1 MHz. The two InN powder samples investigated show different relaxation rates for this signal, consistent with strain-limited tunnelling rates. The hop rate results at higher temperatures shown in figure 9(b) are for the sample having the slower low temperature motion. The amplitude associated with the mobile Mu^+ state in InN grows with temperature, starting below 200 K and includes all the implanted muons above 500 K [14], implying that this signal represents the Mu^+ ground state. The results of figure 9(b) yield a diffusive hop barrier of $\sim$0.4 eV in the onset region for thermally activated motion. The saturation of hop rates at high temperatures implies that this motion is interrupted by trap and release events (see also the later discussion of trapped Mu^+ centres). A more complete description could perhaps be obtained by using depolarization functions for trap and release dynamics (equations (3) and (4)).

We now turn to the dynamics for transitions of a fixed charge state out of a metastable site into its lowest energy state, which may be either localized or diffusively mobile depending on the temperature where the site change occurs. For the Mu^- centres in GaN the $AB_\parallel$-to-

$AB_\perp$ site-change transition is easily identified by the temperature dependence in Ga-related lcr amplitudes and in the amplitudes for the zero-field depolarization signals associated with the two Mu^- states. In figure 5, the circles represent these Mu^- signals, open symbols for the metastable site. There are other transitions feeding into both of these states, but the site change is clearly seen between 450 and 550 K. This particular data set has too few points in that region to give a good measure of the energy required for Mu^- to exit the cage region containing the $AB_\parallel$(Ga) site, but we obtained a metastable-to-stable site-change barrier of 1.51 ± 0.06 eV for Mu^- from similar data [22] on the high concentration Si-doped GaN sample compared to $\sim$1.2 eV from lcr amplitudes [10] in the compensated Zn-doped sample. The low energy Mu^- is already mobile at temperatures where the site change occurs; the motion and transition onset temperatures differ by $\sim$50 K. The relaxation function for the metastable Mu^- centre remains static as the signal amplitude decreases, leading to the conclusion that the $AB_\parallel$ site is not revisited by the mobile Mu^-. Thus, the primary Mu^- diffusion path does not include the $AB_\parallel$(Ga) location.

The lcr and ZF signal for the metastable Mu^- only occur above roughly 200 K. On the basis of the growth step for the metastable Mu^- signal and correlated decrease in the metastable Mu^+ in figure 5, it appears that the trapped Mu^- is formed from a Mu^+ precursor already trapped in the same cage region at the $AB_\parallel$(N) site. We obtained energies of 0.37 eV for the decrease in metastable Mu^+ and 0.25 eV from the increase in metastable Mu^- from the ZF signal amplitudes in figure 5. Presumably those energies are related to changes in lattice distortion and a two step electron-capture process through an intermediate trapped Mu^0 centre. Recall that the results below 50 K suggest the possibility of a shallow Mu^0 precursor to the metastable Mu^+; thus the Mu charge state transitions associated with the 'cage' region in GaN may be quite complicated rather than a simple one-way sequence. One may also note a Mu^+ to Mu^- charge state change for a fraction of the channel $AB_\perp$ centres near 200 K; both steps in this transition give an energy of 0.19 eV. Various other data sets that probe this complicated region of positive to negative charge state conversions each yield two energies between 0.16 and 0.39 eV [10], but without much consistency in assignment and without the obvious separation of these transitions for channel versus cage sites seen in figure 5.

As just discussed, the metastable Mu^+ centre in GaN does not change site before changing its charge state for the n-type samples we examined; thus no useful information on the site-change transitions of Mu^+ could be obtained. In both AlN and InN, the characteristics of trapped Mu^+ centres suggest that they are probably defect related instead of a metastable site intrinsic to the wurtzite structure. Energies associated with site-change transitions out of these Mu^+ trap sites are obtained. For InN depolarization results require at least two different energies to be associated with such transitions, and we are currently attempting to determine whether the zero-field data will support separate signals for two trap sites. The preliminary fits using a single static KT relaxation function ($\Delta = 294$ kHz) for the trapped Mu^+ centres yield energies of $\sim$0.2 and $\sim$0.5 eV from the amplitude switch to the mobile Mu^+ ground state when fit as a two step transition [14]. There are several aspects of the InN data for the Mu^+ states that need further investigation, but what is certain is that a single trap site with a well defined energy can not reproduce these results. When we attempt to use two dynamic KT functions, the only place where the function assigned to trapped states shows any dynamics (other than an amplitude decrease) was above 600 K where the amplitude was nearly zero but grew slightly with increasing temperature. This may be consistent with the hop rate saturation seen for the mobile Mu^+ ground state (figure 9(b)), since both would suggest possible re-trapping at the higher temperatures. Given that the apparent low temperature N–Mu^+ bond reorientation rates are very low in InN based on the signal assigned to Mu^+ ground state, we should leave open the possibility that several distinctly different sites may be separately occupied by Mu^+ in InN

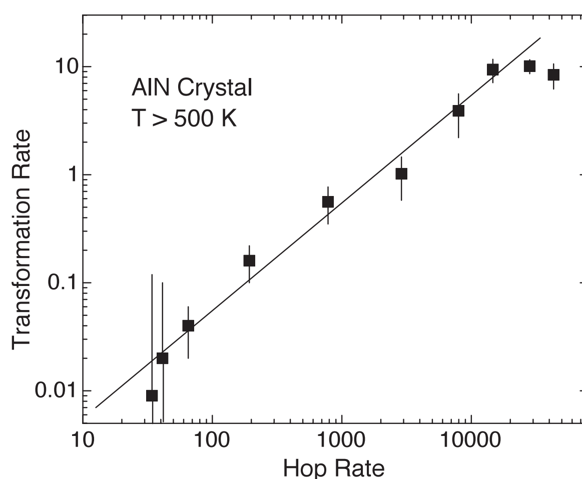

Figure 10. The linear relationship between the motion and conversion rates obtained from the longitudinal relaxation for Mu^0 in AlN implies diffusion-limited trapping.

rather than a dynamic ground state as inferred for GaN and AlN. In that case, the observed dynamics may perhaps involve only sites intrinsic to the wurtzite structure rather than one or more defect-related traps.

We have obtained information on both the formation and dissociation of trapped Mu states in AlN, including data on single-crystal material and films of widely varying quality. An important result from the longitudinal data on single-crystal AlN is that above 500 K, the data require a transition out of Mu^0 with a rate that increases with very similar parameters as the hop rates [15]. In this range, the amplitude of the lcr spectrum from the trapped Mu^+ centre grows rapidly as well as the weakly relaxing longitudinal amplitude in figure 7(b) and the diamagnetic spin precession amplitude. This combination of results suggests trapping of the mobile Mu^0 to form the diamagnetic state seen in the lcr results. Figure 10 demonstrates quite conclusively that the conversion rate of the mobile Mu^0 centre into some other state varies in direct proportion to the Mu^0 hop rate, a result that is consistent with diffusion-limited trapping at a low density defect. The conclusion we reach is that trapping of a mobile Mu^0 in single-crystal AlN produces the same defect centre identified at much lower temperatures in thick film and polycrystalline material and previously assigned [13] to Mu^+ attached to a nitrogen at a defect-related location.

It is noteworthy that all of the signals associated with the trapped Mu state, including the zero-field data of figure 3, are consistent with release from the trap site above roughly 800 K. Zero-field data from several samples [13] with vastly different relative fractions forming this state all yield a dissociation energy very near 1.0 eV (see figure 3(b)) extracted from the motional dynamics version of the KT relaxation function. The fact that the zero-field data imply re-capture at an equivalent location suggests that the trap site responsible might be associated with an extended defect which would have a high density of similar sites nearby. This is also consistent with the fact that amplitudes of the lcr and zero-field signals assigned to the trapped centre are sample dependent and much larger in visually defective thick films compared to polycrystalline material and films without a high density of visible large scale defects. The trap-related signals are large at low temperatures in all samples with a high density of dislocations and exhibiting very large stresses, compared to significant growth only at higher temperatures in bulk single-crystal AlN.

The one defect-related signal for which a specific assignment has been made is the high temperature state shown in figure 5, which begins to grow above roughly 570 K. Both the mobile Mu^+ and mobile Mu^- signals disappear at high temperatures and are replaced by a static KT signal implying a trapped Mu state. This signal is only seen in the Zn-doped GaN sample and does not occur in the undoped or Si-doped material. Therefore, this signal is assigned to a Zn–Mu pair, similar to the passivation complexes found in Zn-doped GaAs and GaP [2, 3]. The Δ for this state is significantly smaller than that for other stationary Mu centres in GaN, consistent with one of its neighbours not having a magnetic moment (only 4.1% of Zn nuclei have non-zero moments). The usual formation mechanism for such a pair is Coulomb capture of a mobile Mu^+ by the ionized Zn^- acceptor, implying a high fraction of Mu^+ centres rather than Mu^- at higher temperatures in this compensated sample. The amplitude for the mobile Mu^+ in figure 5 starts decreasing toward zero at the same point where the Mu–Zn pair signal begins to increase. The mobile Mu^- amplitude also begins to drop at roughly the same temperature, with an increase in slope near 750 K.

We suggest that the features near 750 K may represent a switch in the dominant equilibrium charge state, and thus may identify the temperature where the Fermi level passes through the H^+/H^- equal-population level for thermodynamic equilibrium. This level is predicted [21] to lie about 0.4 eV above mid-gap for GaN, half way between the H[$-$/0] and H[0/+] defect levels, which are separated by $|U| = 1.8$ eV in the latest calculation. In the high concentration Si-doped GaN sample, we obtained [22] an energy of 1.92 ± 0.15 eV for a high temperature transition from mobile Mu^+ to mobile Mu^- states. A lower limit for the energy needed for such a transition should be $|U|$; thus while this interpretation of the experimental features is not definite, it seems to be totally consistent with theoretical results for H in GaN.

6. The Mu model for H in the nitrides

One conclusion that can be drawn from comparing the muonium results with theoretical predictions for hydrogen in the nitrides is that there is very good general agreement. We observe a shallow donor Mu^0 state in InN as predicted. There is non-spectroscopic evidence of atomic-like Mu^0 centres in GaN and AlN, and a shallow neutral that may be present in GaN appears to be associated with a metastable site. Mu^- centres dominate in n-type GaN with amplitudes that increase with increasing electron concentration, as expected. Mu^+ states dominate in AlN and InN, neither of which suffers from the unintended n-type characteristics that are common for GaN. We find that the atomic-like Mu^0 centre in AlN is highly mobile at both low and high temperatures, with a thermal barrier of about 0.7 eV for diffusive motion above 500 K.

Thus far we do not have information on the motional dynamics of all three Mu charge states in any one material. Table 2 summarizes the energies obtained for barriers related to motion and site-change transitions. The general motional behaviour should be common to all three nitrides, but barriers will almost certainly not be identical. The lowest energy Mu^+ centre appears to be mobile at low temperature in each case, consistent with a strong bond with nitrogen and small barriers to reorientational motion as calculated. The characteristics of the low temperature relaxation rates for this state in GaN and AlN imply tunnelling up to at least 350 K. In InN this low temperature Mu^+ motion is slow compared to GaN and AlN, with some possibility that several sites might be separately occupied. The weakly mobile low energy Mu^+ shows thermally activated motion above 350 K in InN with a barrier of about 0.4 eV. This mobile state shows evidence of trapping at defect centres at higher temperatures indicating that this represents diffusive motion. The Mu^+ centres in GaN and AlN show a similar, but poorly characterized, switch to thermal motion. Barrier energies were not determined, but should not be much different than in InN, given the very similar motional-narrowing temperatures. We

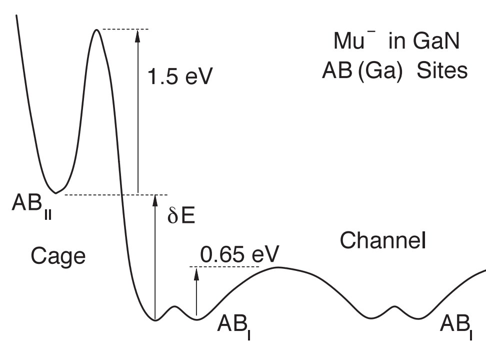

Figure 11. A schematic representation of the energy (enthalpy) relationships for site changes and motion of Mu^- defect centres in GaN. The double minima for $AB_\perp$(Ga) represent three coplanar sites within the wurtzite channels. Similar curves are appropriate for Mu^+ or Mu^0 centres, but the results are less complete.

Table 2. Thermal barriers for motion of the low energy muonium defect centres, and site-change energies for metastable sites or dissociation energies for defect-related trapped Mu states in the III–V nitrides.

	Thermal motion		Site changes		
Material	State	Barrier (eV)	State	Transition	Barrier (eV)
GaN	Mu^-	0.65 ± 0.02	Mu^-	$AB_\parallel \rightarrow AB_\perp$	1.51 ± 0.06
AlN	Mu^0	0.69 ± 0.04	Mu^+	Trap → mobile	1.01 ± 0.04
InN	Mu^+	0.41 ± 0.02	Mu^+	Trap → mobile	0.20 ± 0.01
				Trap → mobile	0.51 ± 0.02

find the $AB_\parallel$(N) site to be metastable for Mu^+ in GaN. Since $AB_\parallel$ is the highest energy bond orientation found in theory, we would expect that site to also be a metastable location for H^+.

We noted differences in Mu^- sites compared to the theoretical results. Experimentally there is a large barrier of about 1.5 eV for Mu^- to escape from the $AB_\parallel$(Ga) site, while that location was not found to give a (meta)stable site in recent theoretical modelling [21]. We find separate $AB_\perp$(Ga) low energy Mu^- sites while theory yields a central site near three $AB_\perp$ locations. We find that Mu^- is thermally mobile among $AB_\perp$ locations with a barrier of 0.65 eV, but that this motion does not include the metastable $AB_\parallel$ location. This conclusion is consistent with the large difference in barriers, and with calculated diffusion paths. Figure 11 shows the energy landscape we infer for Mu^- centres in GaN. The difference in energy between two sites for the same charge state (δE in figure 11) is unlikely to be accessible to μSR experiments. We do not actually have experimental proof that the 0.65 eV barrier produces long range diffusion for Mu^-, as we do for the other two charge states. However, there were features around 150 K in the related Mu^- lcr spectra which we interpreted as a change from sensing an isolated $AB_\perp$ site to local motion among the three closely spaced equivalent sites [12]. The lcr result provides a very rough estimate of $\sim$0.1 eV for the smaller barrier between closely spaced coplanar $AB_\perp$ sites (unlabelled in figure 11).

All of the experimental barriers for motion of Mu centres are considerably smaller that those calculated for diffusion of the equivalent hydrogen centres. This difference is present in most other semiconductors where that comparison has been made. We usually argue that barriers for Mu to escape from a localized site will be smaller than for hydrogen at the same location because of the larger zero-point energy for muonium. Using a model where one

vibrational mode of an oscillator is removed at a transition point, representing the direction of escape, the correction to a barrier due to zero-point motion will be three times as large for Mu as for H. On the basis of typical H vibrational frequencies, or the calculated values in [21], this suggests a reduction of 0.2–0.3 eV for Mu compared to H. Thus, our results would imply barriers of at least 0.6 eV for H^+ thermal diffusion in InN, and 0.9 to 1 eV barriers for H^- in GaN or H^0 in AlN. These numbers are not too different from theoretical results for H^+ and H^0 in GaN, but are somewhat low for H^-.

In conclusion, the experimental results on the muonium centres in the III–V nitrides produce a picture of hydrogen impurities that agrees with the theoretical predictions reasonably well. The tunnelling properties found for Mu^+ and Mu^0 below 300 K should not be as important for hydrogen. On the basis of comparisons for other semiconductors, the sites identified for Mu should provide a very good test of calculated results, while thermal barriers should be considered as a more qualitative comparison. Site localization and barriers for Mu^- represent the largest differences from recent predictions [21]; although even in this case, for the lowest energy sites these differences are a matter of detail and the Mu^- results are qualitatively consistent with theory.

Acknowledgments

This work was supported by the US National Science Foundation, the Robert A Welch Foundation, and the Engineering and Physical Sciences Research Council of the UK.

References

[1] For a review, see Estreicher S K 1995 *Mater. Sci. Eng.* R **14** 319
[2] Chow K H, Hitti B, Kiefl R F, Lichti R L and Estle T L 2001 *Phys. Rev. Lett.* **87** 216403
[3] Lichti R L, Chow K H, Celebi Y G, Davis E A, Hitti B and Cox S F J 2003 *Physica* B **326** 167
[4] Kadono R, Kiefl R F, Brewer J H, Luke G M, Pfiz T, Riseman T and Sternlieb B 1990 *Hyperfine Interact.* **64** 635
[5] Chow K H, Hitti B, Kiefl R F, Dunsiger S R, Lichti R L and Estle T L 1996 *Phys. Rev. Lett.* **76** 3790
[6] Estle T L, Chow K H, Cox S F J, Davis E A, Hitti B, Kiefl R F, Lichti R L and Schwab C 1997 *Mater. Sci. Forum* **258–263** 849
[7] Lichti R L, Chow K H, Hitti B, Davis E A, Sjue S K L and Cox S F J 2001 *Physica* B **308–310** 862
[8] Limpijumnong S and Van de Walle C G 2001 *Phys. Status Solidi* b **228** 303
[9] Cox S F J, Lichti R L and Davis E A 2002 *J. Phys. D: Appl. Phys.* **35** 586
[10] Lichti R L 2003 *Physica* B **326** 139
[11] Lichti R L, Dawdy M R, Head T L, Cox S F J, Hitti B and Schwab C 1999 *Physica* B **273/274** 116
[12] Lichti R L, Cox S F J, Dawdy M R, Head T L, Hitti B, Molnar R J, Schwab C and Vaudo R P 2000 *Physica* B **289/290** 542
[13] Lichti R L, Cox S F J, Davis E A, Hitti B and Sjue S K L 2001 *Physica* B **308–310** 73
[14] Celebi Y G, Cox S F J, Davis E A and Lichti R L 2003 *Physica* B **340–342C** 385
[15] Lichti R L, Celebi Y G, Chow K H, Hitti B and Cox S F J 2003 *Physica* B **340–342C** 430
[16] Cox S F J, King P J C, Williams W G, Chow K H, Jestadt Th, Hayes W, Lichti R L, Schwab C and Davis E A 2002 *Physica* B **289/290** 538
[17] Davis E A, Cox S F J, Lichti R L and Van de Walle C G 2003 *Appl. Phys. Lett.* **82** 592
[18] Lichti R L, Celebi Y G, Cox S F J and Davis E A 2004 *J. Phys.: Condens. Matter* **16** 325
[19] Shimomura K, Kadono R, Ohishi K, Mizuta M, Saito M, Chow K H, Hitti B and Lichti R L 2004 *Phys. Rev. Lett.* **92** 135505
[20] Neugebauer J and Van der Walle C G 1999 *Hydrogen in Semiconductors II* ed N Nickel (San Diego, CA: Academic) p 479
[21] Wright A F, Seager C H, Myers S M, Koleske D D and Allerman A A 2003 *J. Appl. Phys.* **94** 2311
[22] Dawdy M R, Lichti R L, Cox S F J, Head T L and Schwab C 2000 *Physica* B **289/290** 546